

# Energy Confinement and Sawtooth Stabilization by ECRH at High Electron Density in FTU Tokamak

C.Sozzi<sup>1</sup>, S.Cirant<sup>1</sup>, A.Airoidi<sup>1</sup>, G.Bracco<sup>2</sup>, A.Bruschi<sup>1</sup>, P.Buratti<sup>2</sup>, F.Gandini<sup>1</sup>, G.Granucci<sup>1</sup>, A.Jacchia<sup>1</sup>, H.Kroegler<sup>2</sup>, E.Lazzaro<sup>1</sup>, S.Nowak<sup>1</sup>, G.Ramponi<sup>1</sup>, O.Tudisco<sup>2</sup>, B.Angelini<sup>2</sup>, M.L. Apicella<sup>2</sup>, G.Apruzzese<sup>2</sup>, E.Barbato<sup>2</sup>, L.Bertalot<sup>2</sup>, A.Bertocchi<sup>2</sup>, G.Buceti<sup>2</sup>, A.Cardinali<sup>2</sup>, C. Centioli<sup>2</sup>, R.Cesario<sup>2</sup>, S. Ciattaglia<sup>2</sup>, V.Cocilovo<sup>2</sup>, F.Crisanti<sup>2</sup>, R.De Angelis<sup>2</sup>, M.DeBenedetti<sup>2</sup>, B. Esposito<sup>2</sup>, D.Frigione<sup>2</sup>, L. Gabellieri<sup>2</sup>, G.Gatti<sup>2</sup>, E.Giovannozzi<sup>2</sup>, C.Gormezano<sup>2</sup>, M.Grolli<sup>2</sup>, M.Leigheb<sup>2</sup>, G.Maddaluno<sup>2</sup>, M.Marinucci<sup>2</sup>, G.Mazzitelli<sup>2</sup>, P.Micozzi<sup>2</sup>, F.P.Orsitto<sup>2</sup>, D.Pacella<sup>2</sup>, L.Panaccione<sup>2</sup>, M.Panella<sup>2</sup>, V.Pericoli-Ridolfini<sup>2</sup>, L.Pieroni<sup>2</sup>, S.Podda<sup>2</sup>, G.Pucella<sup>2</sup>, G.B. Righetti<sup>2</sup>, F.Romanelli<sup>2</sup>, S.E. Segre<sup>3</sup>, A.Simonetto<sup>1</sup>, P.Smeulders<sup>2</sup>, E.Sternini<sup>2</sup>, N.Tartoni<sup>2</sup>, A.A.Tuccillo<sup>2</sup>, V.Vitale<sup>2</sup>, G.Vlad<sup>2</sup>, V.Zanza<sup>2</sup>, M.Zerbini<sup>2</sup>, F.Zonca<sup>2</sup>

<sup>1</sup>Associazione EURATOM-ENEA-CNR, Istituto di Fisica del Plasma, Milano, Italy

<sup>2</sup>Associazione EURATOM-ENEA sulla Fusione, C.R. Frascati, Frascati, Roma, Italy

<sup>3</sup>INFM and Universit di Roma Tor Vergata Roma, Italy

e-mail contact of main author: sozzi@ifp.mi.cnr.it

**Abstract.** The dependence of the local effective electron thermal diffusivity and of the global energy confinement on the intensity and the distribution of the heat source is explored in ECRH experiments performed on FTU tokamak. Energy transport is analysed by applying a dominant EC heating with  $P_{\text{ecrh}} \approx 0.8$  MW and  $P_{\text{oh}} \approx 0.2$  MW during ECRH, at the frequency of 140 GHz correspondent to the fundamental electron cyclotron resonance at  $B_{\text{tor}} = 5$  T. In order to discriminate the underlying diffusive transport against internal disruptions events, ECRH is also used to stabilize sawteeth. In these conditions, the predominance of ECRH over OH allows a good estimate of heat fluxes. Ion heating in the order of  $T_i/T_e \approx 30\%$  is observed in experiments with central density up to  $10^{20} \text{ m}^{-3}$ .

## 1. Introduction

The peculiar properties of the electron cyclotron heating (ECH), including high power density and wide range of energy deposition profiles in the plasma, allow the modification of current density profiles with the suppression of the sawtooth activity during the flat top of the plasma current. A detailed study of the energy transport properties can be performed in this quiescent condition. In the recent experimental campaign on the FTU tokamak ( $R=0.93$  m,  $a=0.3$  m) the sawtooth suppression has been achieved in a typical deuterium plasma target of  $n_e=0.8-0.9 \cdot 10^{20} \text{ m}^{-3}$  line averaged electron density, 400 kA on the flat top (safety factor at the edge  $\approx 6$ ). Different heating schemes has been successfully employed, using both poloidal steering of the two available EC beams [1] and toroidal field adjustments in the range of 5.4-5.8 T. In this series of discharges up to 850 kW of ECH waves were launched in ordinary polarization from the low field side, in pulses lasting up to 0.5 s. The typical ohmic power ( $P_{\text{ohm}}$ ) of the plasma target was about 420 kW, decreasing at about 200 kW during the EC heating due to the modification of the plasma resistivity with the electronic temperature. The plasma density was sufficiently high to give remarkable effects on e-i coupling and power transfer ( $P_{\text{ei}}$ ). The energy transport analysis, mainly interpretative, has been conducted using the EVITA code that solves the time dependent equations for the poloidal magnetic field and for the electron and ion temperatures. The plasma geometry from equilibrium reconstruction, the electronic temperature from ECE measurements, the plasma line averaged density from DCN and CO<sub>2</sub> laser interferometers, the neutron yield, the visible bremsstrahlung radiation, the radiation losses ( $P_{\text{Rad}}$ ) from bolometric measurements and the calculated power density

deposition of the EC beams ( $P_{EC}$ ) have been used as input data [2]. A consistency check of the calculated quantities was performed comparing calculated and measured neutron yields and loop voltage. The effective electron thermal diffusivity  $\chi_e$  is evaluated from the equation

$$\langle q_e \nabla \rho \rangle = -\chi_e n_e \langle |\nabla \rho|^2 \rangle \frac{\partial T_e}{\partial \rho} \quad (1)$$

where the left-hand term is the normal electron heat flux averaged on the magnetic surfaces of radius  $\rho$ . The heat flux is evaluated from the power balance equation for the electronic population:

$$\langle q_e \nabla \rho \rangle \frac{\partial V}{\partial \rho} = P_{ECH} + P_{Ohm} - P_{ei} - P_{Rad} - \frac{\partial W}{\partial t} \quad (2)$$

where  $V$  is the plasma volume and  $W$  the electron thermal energy.

## 2. Sawtooth stabilization

Sawtooth stabilization was achieved following a few different heating schemes [3]. With a toroidal field  $B_0=5.2$  T (at the vacuum vessel center) and no poloidal injection angle the

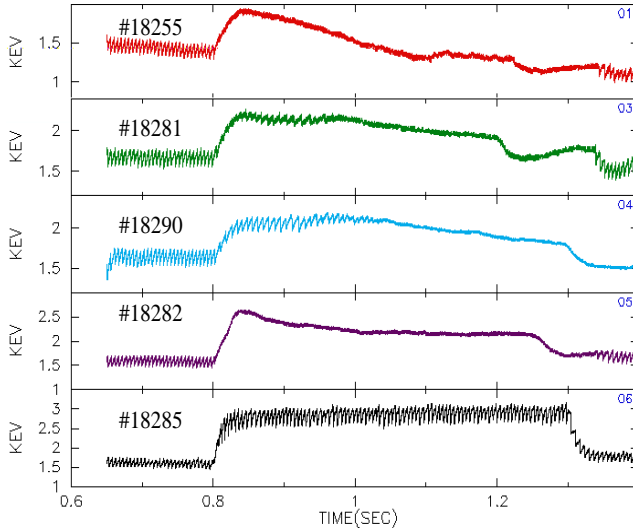


FIG. 1 Electron temperature time traces for different heating schemes.

absorption layer is located on the magnetic axis of the plasma. The shots shown in fig. 1 represent a scan of the toroidal field and of the poloidal angle of injection. Prompt stabilization occurs for #18255 ( $B_0=5.6$ T) where the poloidal angles of launch for the two beams were adjusted to locate the absorption at  $r_{abs}=8$  and 9 cm respectively from the magnetic axis (see fig.2) and for #18282 ( $B_0=5.5$ T,  $r_{abs}=6$  and 10.5 cm). Delayed stabilization occurs for off axis deposition as in #18281 ( $B_0=5.6$ T,  $r_{abs}=9$  and 16 cm) and in #18290 ( $B_0=5.8$ T,  $r_{abs}=10.5$ ). At the level of EC power available, no stabilization occurs if the absorption layer is inside the inversion radius of

the sawteeth, about 5.5 cm from the magnetic axis, as for #18285 ( $B_0=5.4$ T,  $r_{abs}=4$  and 9 cm). The central electron temperature suffers a progressive decreasing starting as soon as sawtooth suppression is achieved. That is due to impurity accumulation at the plasma center, as the rise in the soft x rays and bolometric measurements indicate. A moderate increase of the electron density is also observed. The effect on the global stored energy is negligible for the case of nearly on axis EC deposition (#18255, #18282) but it becomes significant for the off axis case (#18281, #18290). This suggests a relationship with the plasma volume enclosed in EC deposition.

## 3.1 Energy transport analysis

The transport analysis shows that the local electron power balance becomes everywhere negative with the exception of the EC absorption region when EC heating is switched on (see FIG. 3) for both on axis and off axis cases. In the balance also the e-i energy transfer is

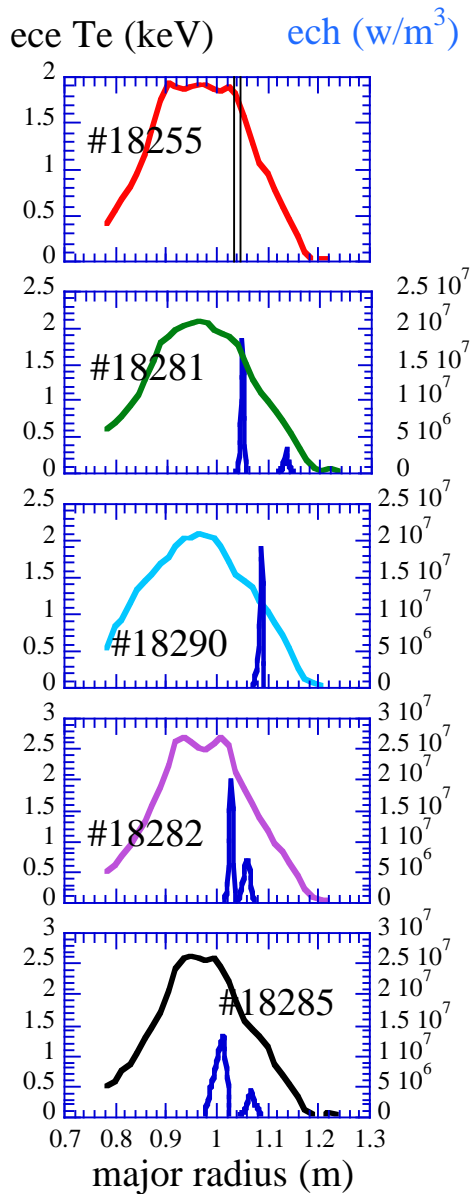


FIG. 2. . Electron temperature profile from ECE and EC power deposition at 30ms after the ECH start for different heating schemes.

kW inside the EC absorption radius), the temperature profile remains peaked, then a certain amount of heat is transferred against the electron temperature gradient. The presence of a step in the diffusivity is a feature relatively independent on the local power density level, since it appears for both the case of beams converging on the same absorption radius (#18290) or not (#18281). Another feature to be considered is the flattening of the magnetic shear profile near the radius of the EC deposition as illustrates FIG.7. For the off axis case, the flattening radius also corresponds to a local minimum in the diffusivity (FIG. 8).

relevant. In #18282 for example the maximum ion temperature increases from 0.91 to 1.15 keV (26%), and the temperatures ratio is  $T_e/T_i=1.6\div 2$ . The experimental neutron flux time behaviour is fitted for a ion thermal diffusivity 4 times larger than neo-classical theory. During the EC heating, the ion population drains from the electrons more power than available from local ohmic heating in the plasma core. A similar consideration holds for the radiation losses in the plasma core, where the radiated power is greater than the local heating source. This effect is clearly visible in the electron temperature profile that appears hollow due to the local negative power balance. Whatever is the main heat transfer process, it appears to be dominant in the local power balance and in shaping the temperature profile.

The ratio between EC power and ohmic one is about 2 at the switching on and it remains almost 4 during the whole EC pulse. The heat flux outside the EC absorption region as far as 2/3 of the radius is therefore mainly due to the EC power, which profile can be evaluated with less uncertainty in respect to the other terms of the power balance equation. This allows a reliable estimate of the effective thermal diffusivity.

As the FIG. 4 shows, the electron diffusivity steps across the EC heating profile, dropping near or below the ohmic value in the inner side and increasing outside. This occurs apparently regardless of the position of the EC absorption in the plasma column. This process is switched on in a very short time scale (few ms) at the EC heating start, and lasts along the whole pulse. FIG. 5 shows this calculation for #18290. In spite of negative local power balance in the core of the plasma (about 200

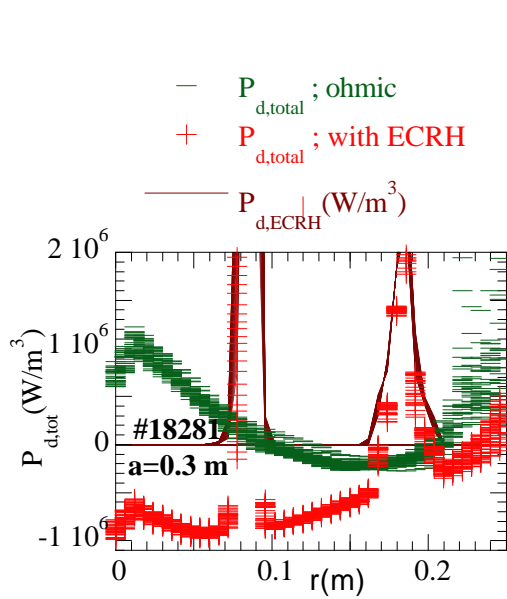


FIG. 3 Local power balance for #18281

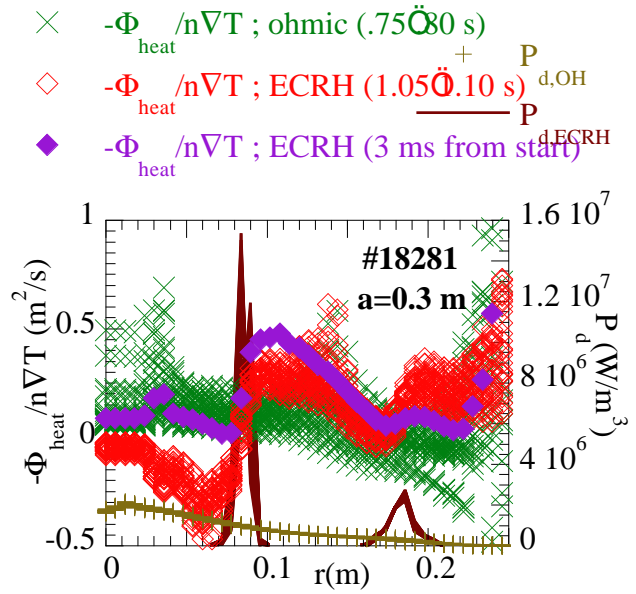


FIG. 4 Electron thermal diffusivity and power sources for #18281

### 3.2 Evaluation of the power balance errors

In order to estimate possible causes of error in the thermal diffusivity calculation due to uncertainty about the source and sink terms, the heat flux was evaluated supposing the maximum possible error in the location of the EC heating profile, and the power density was accordingly changed preserving the total EC power. Moreover, the shape of the deposition profile was broadened and sharpened. The main features of the diffusivity profile remain unchanged. Since the negative part of the diffusivity profile is located in the inner side of the plasma in respect to the deposition profile, also an error up to 100% in the ohmic and

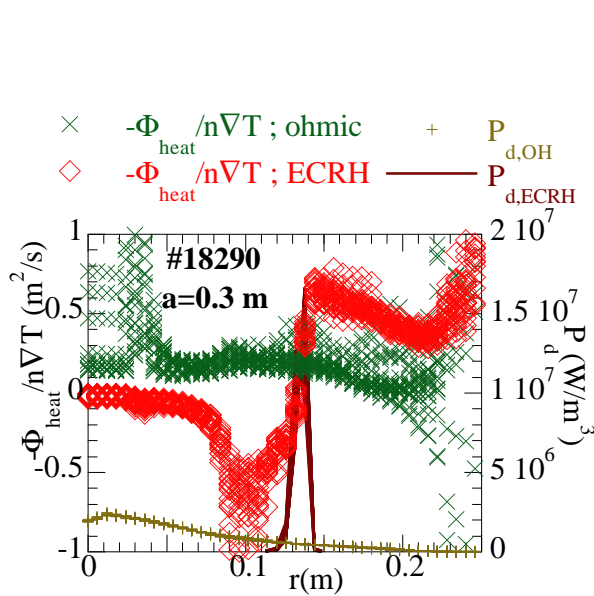


FIG. 5 Electron thermal diffusivity and power sources for #18290

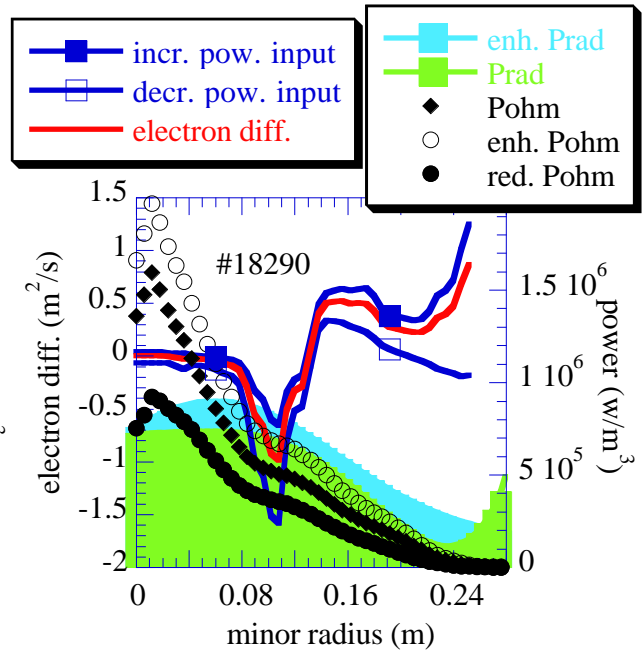


FIG. 6 Evaluation of the power balance error due to ohmic and radiation uncertainties (#18290)

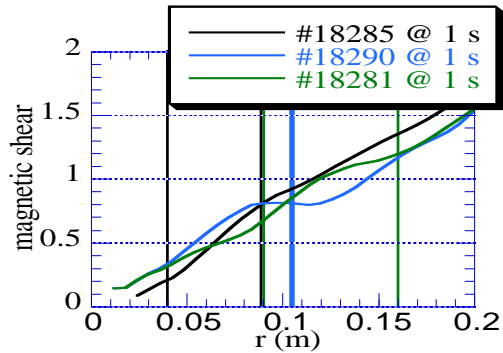


FIG.7. Magnetic shear. Vertical lines mark the absorption radius.

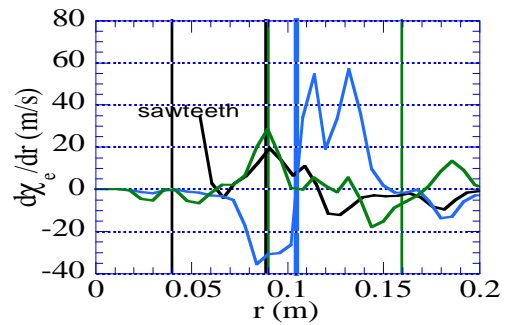


FIG.8. Derivative of the electron thermal diffusivity

radiation power densities in the center were supposed. The range of this variation of source and sinks terms has been chosen maintaining a reasonable agreement with the experimental data, line or volume integrated. Results of this calculation are shown in figure 6 for #18290. Also in this case the main features of the diffusivity profiles are unchanged and it is particularly clear for #18290 that it still goes negative.

#### 4. Conclusions

Stabilization of the sawtooth activity in plasma scenarios with high electron density is achieved if  $P_{EC} > P_{OH}$  and the absorption is outside the inversion radius. The impurity accumulation starting in the plasma core after stabilization and the electron-ion thermal exchange limit the electron temperature peaking. The analysis of the energy transport has been performed for moderate and significant off axis EC deposition. Due to the decreasing of the ohmic input at the ECH switch-on the power balance becomes everywhere negative except that in the deposition region. In all cases studied the effective electron thermal diffusivity presents a clear step across the deposition region, decreasing inward and increasing outward. In cases with strongly localized off axis ECH deposition evidence of energy transport against the electron temperature gradient is found.

Presence of effects due to heat transfer not driven by temperature gradient were early suggested in [4] and recently in [5,6], but the understanding of its physical mechanism is still an open question.

- [1] C.Sozzi, et al., "High Power System for ECRH at 140Ghz, 2MW, 0.5s on FTU Tokamak". 13th Topical Conf. on Appl. of Radio Frequency Power to Plasmas, April 12-14, 1999, Annapolis, Maryland, AIP Conf.Proc. 485 pp. 462-465
- [2] S.Nowak, et al. "40 Ghz EC waves propagation and absorption for normal/oblique injection on FTU Tokamak" 13th Topical Conf. on Appl. of Radio Frequency Power to Plasmas, April 12-14, 1999, Annapolis, Maryland. AIP Conf.Proc. 485 pp. 466-4692]
- [3] S.Cirant, et al. "Sawteeth stabilization and ion temperature enhancement by localized ECRH in FTU plasmas" Proceedings of 25th EPS Conference on Controlled Fusion and Plasma Physics, Praha, European Physical Society, July 1998, ECA Vol 22C (1998) pp 1174-1177
- [4] T.C.Luce, et al, Phys. Rev.Lett.68, 52 (1992).
- [5] P.Mantica, et al "Heat convection and transport barriers in low magnetic shear RTP plasmas" Phys. Rev.Lett, to be published.
- [6] S.Cirant, A.Airoidi, L.Bertalot et al., 26th EPS Conference on Controlled Fusion and Plasma Physics, Maastricht, June 1999, Plasma Phys. Contr. Fusion 41B 351 (1999)